http://doi.org/10.1590/1678-992X-2021-0202

ISSN 1678-992X

SCIENTIA AGRICOLA

Research Article

Foliar application of graphene oxide, Fe, and Zn on *Artemisia dracunculus* L. under salinity

Mohammad Bagher Hassanpouraghdam[1]*, Lamia Vojodi Mehrabani[2], Nahideh Kheirollahi[2], Amir Soltanbeigi[3], Leila Khoshmaram[4]

[1]University of Maragheh/Faculty of Agriculture – Dept. of Horticultural Science, P.O. Box 83111-55181 – Iran – Islamic Republic.
[2]Azarbaijan Shahid Madani University/Faculty of Agriculture – Dept. of Agronomy and Plant Breeding, P.O. Box 53751-71379 – Tabriz – Iran – Islamic Republic.
[3]Afyonkarahisar Health Sciences University/Faculty of Pharmacy – Dept. of Basic Pharmaceutical Sciences, Dörtyol Mahallesi 2078 Sokak, 3 – Afyonkarahisar – Turkey.
[4]Azarbaijan Shahid Madani University/Faculty of Science – Dept. of Chemistry, 53751-71379 – Tabriz – Iran – Islamic Republic.
*Corresponding author <hassanpouraghdam@gmail.com>

Edited by: Leonardo Oliveira Medici

Received August 30, 2021
Accepted December 16, 2021

ABSTRACT: Salinity is an abiotic stressor that greatly influences crop growth and yield. Scientists are always exploring diverse methods to combat salinity depression. Here, we conducted a greenhouse experiment to study the effects of NaCl salinity (0, 50, and 100 mM) under the foliar spray with zinc-oxide, nano zinc-oxide, iron-chelate, magnetized-Fe, and graphene-oxide on tarragon. The results revealed that the treatment with foliar spray of graphene showed the highest K^+/Na^+. Salinity of 50 and 100 mM × all foliar applications increased superoxide dismutase activity, whereas 100 mM NaCl raised the malondialdehyde content to its highest level. All salinity levels × Zn foliar spray improved the catalase activity. The foliar spray and salinity experiment exposed to Zn-treated plants attained the highest contents of essential oils. Proline and total phenolics showed the greatest amounts with 50 and 100 mM of NaCl, respectively. The GC/MS analysis revealed 38 compounds in the oil of *Artemisia dracunculus* L. as estragole (81-91.8 %) was the most dominant constituent. The highest amounts of estragole were found at 50 and 100 mM NaCl foliar sprayed with ZnO. Cis-Ocimene (0.1-6.4 %) was another major constituent with a high variation between the treatments. The highest cis-ocimene content was recorded at 100 mM NaCl × foliar Fe-chelated and in the graphene treatment. Overall, salinity adversely affected the physiological responses of tarragon; however, foliar spray with both forms of Fe and Zn partially ameliorated the adverse salinity effects.

Keywords: malondialdehyde, tarragon, essential oil, antioxidant enzymes

Introduction

Salinity has adverse effects on plant growth and crop yield mainly because it generates excessive reactive oxygen species (ROS) (Munns and Tester, 2008; Gohari et al., 2020a). Under salinity, sodium (Na^+) accumulation in sensitive metabolic sites may compromise the activity of enzymes in the Calvin cycle, the phenylpropanoid pathway, and glycolysis. The maintenance of ionic homeostasis and the stability of cell membranes are directly associated to adequate plant nutrition under salinity (Zhao et al., 2020; Guo et al., 2020). Salinity also influences ions homeostasis by affecting gene expression and creating a cascade of events, diverting a pool of metabolites to withstand the stressor impacts. The SOS and NHX are the two major genes involved in ionic homeostasis under salinity (Wu et al., 2004; Nieves-Cordones et al., 2010; Guo et al., 2020). The appropriate availability of essential minerals, such as iron (Fe) and zinc (Zn), drastically fortifies plant tolerance to stress under saline conditions. Zn has structural and functional roles in cell membrane integrity (Marschner, 1995) and plays a crucial role in detoxification and control of free radicals, damaging fatty acids and sulfhydryl residues in the cell membranes (Marschner, 1995). Likewise, Fe bears crucial roles in the activity and dynamics of several enzymes, in chlorophyll formation, in photosynthesis, and in transpiration (Vojodi Mehrabani et al., 2018; Kanjana, 2019; Hassanpouraghdam et al., 2019).

Currently, issues related to environmental pollution have placed the use of nano-fertilizers as a promising alternative to improve crop yield. Chelating the minerals makes coalitions stable between the chelating media and the minerals, thus greatly reducing the use of fertilizers while improving plant yield (Pandey et al., 2018; Etesami et al., 2021). In plants, graphene-oxide (GO) serves as a carrier for several compounds inside the cells and helps plant growth by promoting the translocation of amino acids (Deng and Berry, 2016; Mahmoud and Abdelhameed, 2021). Therefore, GO under stressful environments increases plant growth potential by enhancing the contents of chlorophylls and by improving photosynthesis efficiency (Safikhan et al., 2018; Mahmoud and Abdelhameed, 2021).

Artemisia dracunculus L. (tarragon) is a perennial herbaceous aromatic plant of the Asteraceae family (Kordali et al., 2005). Tarragon is a source of minerals, vitamins, and essential oils (Kordali et al., 2005; Obolskiy et al., 2011). This study assessed the foliar treatment of GO, Zn, and Fe on the physiological responses of tarragon under stressful saline conditions.

Materials and Methods

Plant material and experimental setup

We assessed the effects of NaCl salinity and the foliar application of zinc-oxide, nano-zinc-oxide, FeEDTA, nano-iron (magnetic-iron) and GO on the growth and physiological responses of *A. dracunculus*. We conducted

a factorial experiment based on a randomized complete block design with three replications. Standard ambient light provided a light intensity of about 450 µmol m^{-2} s^{-1}. The temperature regime was 25 and 20 °C at day and night, respectively, and the relative humidity was 65 %.

A. dracunculus rhizomes, homogenous in size and diameter, were transferred to the greenhouse and acclimatized during one month with the modified Hoagland's nutrient solution (EC 2.1 mS cm^{-1}; pH = 5.8). Plantlets were grown in pots (5 L) containing medium-sized perlite in an open soilless culture system.

Salinity treatments (0, 50, and 100 mM by adding adequate NaCl) were added to the Hoagland's nutrient solution when plants had three-four leaves after four weeks of planting. The salinity levels began with 25 mM and were gradually increased to reach the final level (100 mM after two weeks). To avoid salinity accumulation, pots were washed with tap water once a week. Six treatment solutions were used, including dH_2O (control), zinc oxide and its nano form at 3 mg L^{-1} (Vojodi Mehrabani et al., 2018), FeEDTA, and nano-iron at 3 mg L^{-1} (Hassanpouraghdam et al., 2019) as well as GO (0.05 g L^{-1}) (Begurn et al., 2011). Zinc oxide and nano-ZnO were supplied by a nano company from the United States. Nano-Fe and GO were synthesized according to the methods described below. The first foliar application was carried out simultaneously with the increase in salinity levels. The second application occurred two weeks after. Plants were harvested nine weeks after the beginning of salinity treatments. The optimal pH (5.8) of the nutrition solution (NS) was recorded every other day and adjusted accordingly by using H_2SO_4 (5 % v/v). This experiment consisted of 18 treatment combinations with 108 pots. Two pots were considered as an experimental unit.

Instrumentation

The fourier-transform infrared spectroscopy (FT-IR) spectrum of GO and Fe_3O_4 nanoparticles were recorded on a Vector 22 instrument using potassium bromide (KBr) as the mulling agent. The X-ray diffraction analyses (XRD) of GO and Fe_3O_4 nanoparticles were conducted on Bruker D8 Advance instrument with Cu-K_α radiation source (1.54 Å) between 8 and 80° generated at 35 mA and 40 kV at room temperature. The morphology identification of GO was carried out under a scanning electron microscope. Furthermore, a heater and an ultrasonic bath helped in the different steps of the synthesis process.

Synthesis of GO and Fe_3O_4 magnetic nanoparticles (MNP_S)

The modified Hummers method (Nakajima et al., 1988) was used to prepare graphene oxide from graphite powders. In brief, 10 g of graphite powder and 5 g of $NaNO_3$ were added to 230 mL of concentrated H_2SO_4. Then, to prevent overheating and explosion, $KMnO_4$ (30 g) was gradually added to the solution with constant stirring and cooling. The solution was kept standing overnight at room temperature. On the next day, the solution was transferred to 500 mL boiling H_2O to form graphite oxide. Finally, GO was washed with ethanol and dried at 70 °C for 24 h.

For the synthesis of Fe_3O_4 magnetic nanoparticles (MNPs), 50 mL of deionized water was degassed into an ultrasonic bath for 10 min and added to 4.86 g iron (III) chloride hexahydrate ($FeCl_3 \times 6H_2O$) and 3.34 g iron (II) sulfate heptahydrate ($FeSO_4 \times 7H_2O$). The solution was heated to 100 °C and vigorously stirred to dissolve the iron. Then, 12 mL concentrated ammonia solution was rapidly added under vigorous stirring to complete the reaction (2 h) and to form black iron oxide MNP_S. The formed Fe_3O_4 MNPs were cooled at room temperature and collected using a magnet. Later, Fe_3O_4 MNPs were first washed with a mixture of ethanol: water (50:50, v/v) and then with pure ethanol. Finally, Fe_3O_4 MNPs were dried at 80 °C for 5 h in an oven.

Characterization of GO and Fe_3O_4 MNPs

The FT-IR spectrum of GO (Figure 1A) shows a broad peak around 3400 cm^{-1} in the high-frequency area related to the stretching vibration of OH groups of water molecules adsorbed in GO with strong hydrophilicity. The absorption peaks at 2923 cm^{-1} and 2853 cm^{-1} represent the symmetric and anti-symmetric stretching vibrations of CH_2, while the presence of the absorption peak observed in the medium frequency area, at 1628 cm^{-1}, can be attributed to the stretching vibration of C = C and C = O of carboxylic acid groups at the edges of GO (Shahriary and Athawale, 2014). Moreover, the peak at 1384 cm^{-1} shows the C-O of carboxylic acid. These oxygen-bearing groups reveal GO. The polar hydroxyl groups generate hydrogen bonds between graphite and water molecules, manifesting the hydrophilic nature of GO. The XRD outcome of GO is shown in Figure 1B. The scanning electron microscopy (SEM) image of synthesized GO is given in Figure 1C. The figure clearly shows that GO has a layered structure containing ultra-thin and homogeneous graphene films.

The FT-IR spectrum of Fe_3O_4 MNPs shows a strong peak at around 582 cm^{-1} possibly related to the Fe-O bond in Fe_3O_4 (Figure 1D). This peak was shifted to a high wave number compared to the Fe-O bond peak of bulk magnetite at 570 cm^{-1} due to the NPs size (Camel, 2003), showing that the Fe_3O_4 MNPs were successfully synthesized. The X-ray diffraction pattern (XRD) of Fe_3O_4 MNPs is presented in Figure 1E. The diffraction peaks in 2θ region of 5-80° (30.007, 35.601, 43.239, 53.782, 57.372, and 63.058°) are marked by their indices (220, 311, 400, 422, 511, and 440), which confirmed the formation of Fe_3O_4 MNPs (Camel, 2003).

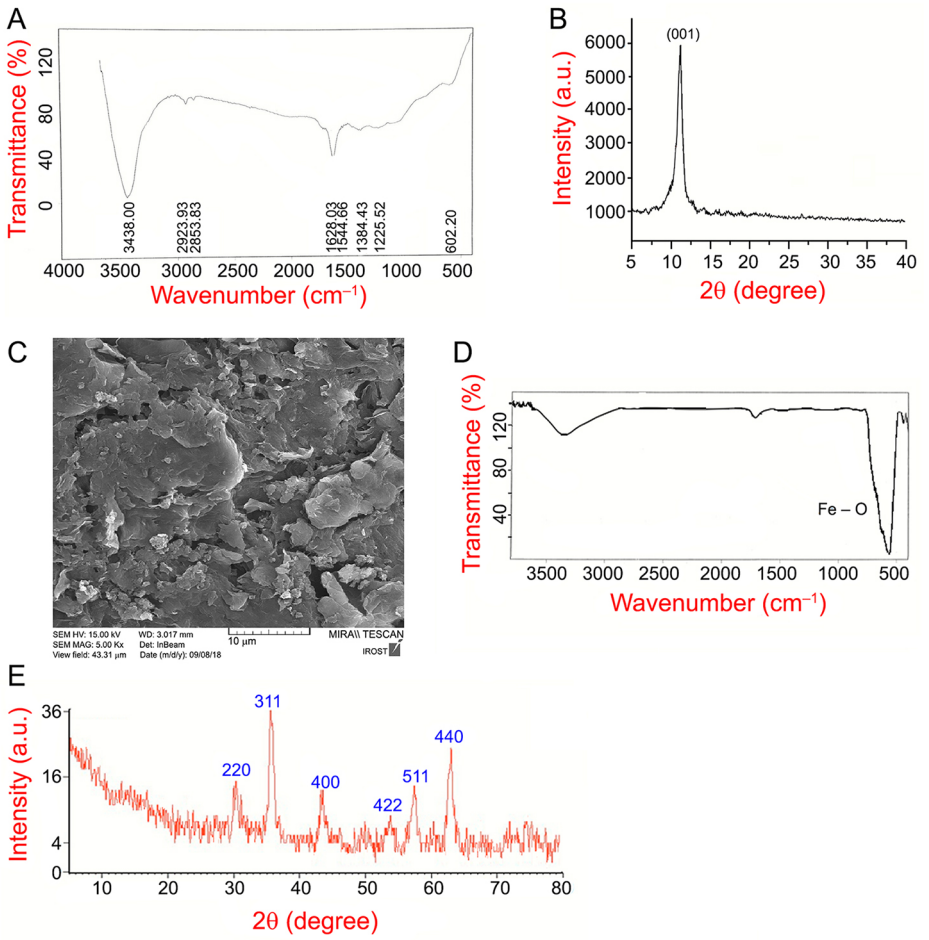

Figure 1 – Fourier transform infrared spectroscopy (A), X-ray diffraction analysis (B), and scanning electron microscope image (C) of graphene oxide as well as FT-IR spectrum (D) and XRD pattern (E) of Fe3O4 MNPs, respectively.

Fresh and dry weight of plants (biomass)

Plant parts harvested early in the flowering time (nine weeks after planting) were air-dried until constant weight. Fresh and dry weights were recorded on a digital scale.

Total phenolics content

The total phenolics content was determined according to Kim et al. (2006) using the Folin-Ciocalteu method.

Total flavonoids content

The total flavonoids content was measured according to Quettier-Deleu et al. (2000).

Proline content

The proline content was obtained according to the method described by Fedina et al. (2006).

Elemental composition

The minerals in the leaves were analyzed by the method described in detail by Chrysargyris et al. (2018). The flame photometric method quantified sodium (Na^+) and potassium (K^+). The Zn and Fe content of plant tissues were traced by the atomic absorption spectroscopy using the method of Honarjoo et al. (2013).

Determination of malondialdehyde (MDA) content

Malondialdehyde was quantified according to Nareshkumar et al. (2015) at 520 nm.

Catalase (CAT) and superoxide dismutase (SOD) activity

To measure the SOD activity, 0.2 g of fresh leaf tissue was homogenized in phosphate buffer (pH 6.8, 4 °C) and centrifuged for 15 min at 17000 g under 4 °C. The supernatant was used for the SOD activity analysis

using the method developed by Giannopolitis and Ries (1997). For the CAT activity, 0.2 g of fresh leaf tissue was blended with 0.1 M potassium phosphate (1:2 w/v, pH 7). After filtration, the solution was centrifuged at 12000 g for 30 min at 4 °C. After, 0.2 mL of the extract was mixed with 1 mL of reaction solution containing 65 mM H_2O_2 and 60 mM sodium-potassium phosphate buffer (pH 7.4, 25 °C at 4 min). The enzyme activity stopped with 1 mL of 32 mM ammonium molybdate and the solution color change was recorded at 405 nm (Luhova et al., 2003).

Essential oils (EOs) extraction

The EOs were extracted from 30 g of dry plant tissues by hydro-distillation for 3 h using a Clevenger-type apparatus. The oils were dehydrated using anhydrous sodium sulfate.

GC-MS analysis

Gas chromatography (Agilent Technologies, 7890B), equipped with a flame ionization detector (FID) and linked to a mass spectrometer (Agilent Technologies, 5977A), was used for the oil components analysis. The oil constituents were separated by an HP-Innowax column (Agilent 19091N-116: 60 m × 0.320 mm internal diameter and 0.25 µm film thickness). The column was held initially at 70 °C for 5 min then increased to 160 °C with 3 °C min^{-1} intervals. Later, the temperature reached 250 °C with a 6 °C min^{-1} gradual increase and 5 min hold time. Helium (99.9 % purity) was the carrier gas (1.3 mL min^{-1} flow rate). The injection volume was 1 µL (20 µL oil in 1 mL n-Hexane). The solvent delay time was 8.20 min. The split mode of 40:1 was used for injection. The detector, injector, and ion source temperatures were 270 °C, 250 °C, and 270 °C, respectively (Figure 2). The mass scan range was (*m/z*): 35-450 AMU under electron impact (EI) ionization of 70eV.

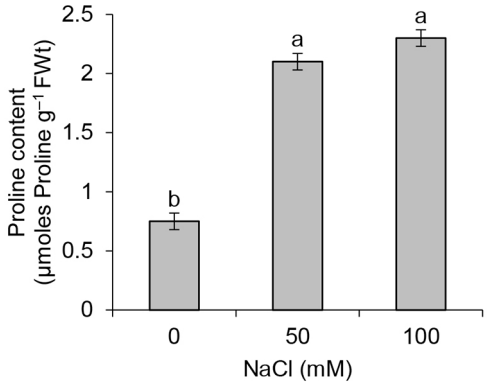

Figure 2 – Mean comparison for the effects of NaCl salinity (0-50 and 100 mM) on the proline content of *Artemisia dracunculus* plants grown in perlite. Differences ($p < 0.01$) between treatments are indicated by the diverse Latin letters

The retention indices were acquired by the simultaneous injection of n-alkanes (C7-C30/Sigma-Aldrich) on the HP-Innowax column by GC/FID system. The volatile oil constituents were identified by comparing the retention indices and the mass spectra data by the computer library search database of NIST, Wiley libraries, other published mass spectral databases, and the related literature review (Adams, 2007).

Experimental design and data analysis

The experiment was factorial based on Randomized Complete Block Design (RCBD) with three replications. The means were compared by the Duncan's multiple range test at 1 and 5 % probability levels. The data normality was tested by SPSS (version 20) and in case of any abnormal data, the chi-square conversion test was used.

Results and Discussion

Proline content

The proline content was responsive to 50 and 100 mM salt stress ($p < 0.01$) and 100 mM salinity had 78 % more proline content than the control treatment (Figure 2). Under saline conditions, the production of low molecular weight solutes, such as proline, glycine-betaine, salicylic acid, and melatonin, is fundamental to ensure the osmotic homeostasis in glycophytes (Antoniou et al., 2016). The role of proline in osmotic potential regulation is connected toprotecting phospholipid membranes, reducing the deteriorative effects of excessive ROS production (Santander et al., 2019). Glutamate is a precursor for the biosynthesis of both chlorophyll and proline. Under saline environments, glutamate is more directed to the proline biosynthesis and thus the chlorophyll biosynthesis and function are adversely impacted (Drazkiewicz, 1994). Proline accumulation in the plant under salinity depends on the upstream regulation of P_5C_5 genes (glutamate pathway) and on the downstream regulation of proline dehydrogenase genes (Mansour and Ali, 2017; El Mokhtari et al., 2020). The proline biosynthesis is also associated to the protection of the Rubisco enzyme and the electron transfer chain in the complex II of mitochondria (Mansour and Ali, 2017; El Mokhtari et al., 2020).

Whenever necessary, proline could be a C and N source and prevent the absorption of Na^+ and Cl^- by the melioration of plant tolerance to stress via the activation of the Salt Overly Sensitive (SOS) pathway (Rady et al., 2011; Chrysargyris et al., 2018; Guo et al., 2020). Accordingly, exposure to 150 mM NaCl stimulated (57 %) proline accumulation in rosemary (Hassanpouraghdam et al., 2019) and (80 %) in peppermint compared to control plants (Askary et al., 2017). The decrease in the proline content showed adverse salinity effects on grapevine plants (Gohari et al., 2021). In our experiment,

foliar treatments had no significant effect on the proline content of plants; however, the foliar treatment of Fe and Zn reduced proline content under 150 mM salinity in peppermint and rosemary (Askary et al., 2017; Hassanpouraghdam et al., 2019).

Essential oils content

The essential oils (EOs) content was affected by the interaction of salinity × foliar treatments ($p < 0.01$). The highest EOs content was found in the treatments of no salinity × all spray, 50 mM salinity × foliar spray with ZnO, and 100 mM salinity × foliar application of nano-Zn and ZnO (Table 1). Therefore, under saline stress, foliar application of ZnO and nano-Zn positively effected the EOs content. The lowest EOs content was recorded for $NaCl_{50}$ × nano-Fe (44 % lower than the control). The $NaCl_0$ × GO contained the highest EOs content (52 % more than the control). There was no difference in the EOs content between $NaCl_{100}$ × nano-Zn, $NaCl_0$ × nano-Fe, and $NaCl_{100}$ × FeEDTA. However, $NaCl_0$ × nano-Zn contained 21 % less oil accumulation compared to $NaCl_0$ × GO. The GO stimulated the biosynthesis of Indole-3-Acetic Acid (IAA) and thus root growth, mitigating the destructive effects of salinity due to the reduced ROS production (Cheng et al., 2016; Ren et al., 2016). Auxin promotes the plant growth potential and especially develops the root system, thus enhancing the biosynthesis and accumulation of secondary metabolites (Ren et al., 2016). The EOs content of *Lavandula angustifolia* plants was negatively responsive to $NaCl_{100mM}$ × Zn foliar application (Chrysargyris et al., 2018). Under these conditions, Zn foliar spray had 35 % less effect on *L. angustifolia* oil content than control plants. Presumably, foliar spray with nutritional elements increased the oil content by the improved photosynthesis potential and a balanced sink-source relationship (Hassanpouraghdam et al., 2010; Chrysargyris et al., 2018). Zn plays a crucial role in photosynthesis and in the general metabolism, increasing the EOs content in plants (Marschner, 1995; Hassanpouraghdam et al., 2010). Fe is another essential nutrient with critical roles in the activity of several enzymes in N fixation, photosynthesis, and respiration. Improvements in overall plant metabolism helps plant growth and the EOs biosynthesis (Marschner, 1995; Askary et al., 2017; Hassanpouraghdam et al., 2019). The high activity of nano elements possibly makes them good candidates to enhance metabolic reactions, compared to their common forms.

Malondialdehyde content

The malondialdehyde (MAD) content was affected by the interaction of salinity and foliar applications. The greatest MAD content was observed in $NaCl_{100\ mM}$ × no foliar spray, indicating the deteriorative action of salinity on cell membranes. The MDA content also increased as salinity increased to 50 and 100 mM. Under salinity, foliar treatments reduced the MDA content, reaching minimum values under $NaCl_{50}$ × nano-Fe (58 % lower MDA content compared to $NaCl_{100}$ × nano-foliar spray). The foliar spray has a positive effect on the maintenance of cell membranes integrity in no-saline conditions, where all foliar applications reduced the MDA content (Table 1). Salinity adversely affects the integrity of membranes. The damage of membranes is observed by the increased ion leakage (Safikhan et al., 2018). The high concentrations (500 mg L^{-1}) of GO restricted maize plants growth due to the over-production of ROS radicles in the root tissues, causing damage to cells and excessive electrolyte leakage and MDA accumulation (Ren et al., 2016). The GO treatments at 1600 mg L^{-1} had a positive role in the MDA content of plants; however, lower dosage (100 mg L^{-1}) reduced the MDA content in faba bean (Anjum et al., 2014). More than 100 mg L^{-1} of GO was toxic to plants, causing breakage of cell membranes and accelerated ion leakage as well as lipids and proteins peroxidation. Nevertheless, low GO concentrations can improve plant growth by reducing H_2O_2 generation and lessening lipid and protein peroxidation (Anjam et al., 2014). Salinity increased the MDA and H_2O_2 contents in rosemary and *Ocimum basilicum*. However, foliar spray with nano-Fe and Zn reduced the amount of both compounds mainly due to the reduced levels of ROS molecules (Hassanpouraghdam et al., 2019; Gohari et al., 2020b). Similar results on the reduction of the MDA content in response to the salinity × foliar Fe, Zn, and GO applications were recorded in comparison to the sole effects of 50 and 100 mM salinity levels, indicating the efficacy of foliar treatments to keep cell membranes intact and prevent over-accumulation of MDA molecules under salinity (Safikhan et al., 2018; Hassanpouraghdam et al., 2019). Zn stimulates the phenolic contents in plants, improving the integrity of membranes, increasing the content of metallothioneins, preserving the structural compounds, and preventing unwanted reactions between Fe and other metal elements in cells (Lingyun et al., 2016).

Catalase activity

Salinity × foliar applications influenced the Catalase (CAT) activity in tarragon. The highest CAT activity was found in the control, in 100 mM NaCl × foliar application of nano-zinc and zinc oxide, and in 50 mM NaCl × nano-Zn (Table 1). Under salinity, the $NaCl_{100}$ × nano-Zn (41.3 unit mg^{-1} protein min^{-1}) treatment exhibited 10.4 % more CAT activity than $NaCl_{100}$ × ZnO. There was no difference ($p > 0.01$) between $NaCl_{50}$ × nano-Zn (39.6 unit mg^{-1} protein min^{-1}) and $NaCl_0$ × nano-Zn (39.3 unit mg^{-1} protein min^{-1}). In *Vigna radiata* L., foliar application of Zn (25 µM) under salinity of 150 and 200 mM increased the CAT and SOD activities (Al-Zahrani et al., 2021). Ahmad et al. (2017) reported a similar result. The results of these experiments are in line with the findings of our study. Conversely, in peppermint, 50 mM salinity increased the CAT activity; however,

Table 1 – Interaction effect of salinity (0, 50, and 100 mM NaCl) and foliar applications (no foliar, ZnO, nano-ZnO, FeEDTA, magnetic-Fe and graphene oxide) on the essential oils content, catalase activity, malondialdehyde content, superoxide dismutase activity, Zn content, and K/Na ratio of *Artemisia dracunculus* plants grown hydroponically in perlite.

NaCl Salinity	Foliar application	Essential oil content	Malondialdehyde content	Catalase activity	Superoxide dismutase	K^+/Na^+ ratio	Zn
nM		%	μm g^{-1} Fwt	unit mg^{-1} protein min^{-1}	μm g^{-1} protein		mg g^{-1}
0	No foliar	1.6^{a-c}	0.66^{f}	35.3^{b-e}	7.3^{e}	18.1^{b}	6.6^{f}
0	Zinc oxide	1.7^{ab}	0.46^{f}	37.6^{a-c}	9.6^{de}	22.8^{b}	32.0^{a}
0	Nano-zinc oxide	1.5^{a-c}	0.46^{f}	39.3^{ab}	14.3^{b-e}	23.0^{b}	36.5^{a}
0	Fe EDTA	1.8^{ab}	0.4^{f}	33.0^{c-e}	11.0^{c-e}	22.7^{b}	9.1^{ef}
0	Magnetic Fe	1.8^{ab}	0.46^{f}	31.3^{ef}	12.6^{b-e}	28.9^{b}	8.5^{ef}
0	Graphene	1.9^{a}	0.46^{f}	28.0^{fh}	13.6^{b-e}	57.1^{a}	21.1^{bc}
50	No foliar	1.2^{c-e}	2.7^{b}	27.6^{fh}	18.0^{a-e}	0.77^{c}	5.6^{f}
50	Zinc oxide	1.6^{a-c}	2.1^{cd}	35.3^{b-e}	23.3^{a-d}	0.75^{c}	25.2^{b}
50	Nano-zinc oxide	1.0^{e}	1.9^{de}	39.6^{ab}	26.6^{ab}	0.95^{c}	25.3^{b}
50	Fe EDTA	1.3^{c-e}	1.8^{de}	30.6^{e-g}	31.2^{a}	1.1^{c}	4.8^{f}
50	Magnetic Fe	0.9^{e}	1.6^{e}	35.6^{b-e}	24.3^{a-c}	1.2^{c}	5.0^{f}
50	Graphene	1.1^{d-e}	1.7^{de}	32.3^{d-f}	24.4^{a-c}	1.4^{c}	14.2^{de}
100	No foliar	1.3^{c-e}	3.8^{a}	24.3^{h}	31.0^{a}	0.31^{c}	4.3^{f}
100	Zinc oxide	1.6^{a-c}	2.6^{b}	37.0^{a-d}	26.3^{ab}	0.35^{c}	19.7^{b-d}
100	Nano-zinc oxide	1.8^{ab}	2.5^{bc}	41.3^{a}	31.3^{a}	0.36^{c}	19.1^{b-d}
100	Fe EDTA	1.5^{b-d}	2.2^{cd}	34.6^{b-e}	25.1^{a-c}	0.40^{c}	7.1^{f}
100	Magnetic Fe	1.2^{c-e}	2.6^{b}	31.0^{d-f}	24.5^{a-c}	0.43^{c}	5.2^{f}
100	Graphene	1.2^{c-e}	2.5^{bc}	26.3^{gh}	19.0^{a-e}	0.55^{c}	15.6^{cd}

Differences between treatments are indicated by the diverse Latin letters ($p < 0.01$ except for essential oils content in which p was < 0.05).

foliar spray with nano-Fe reduced the CAT activity and simultaneously improved the SOD activity (Askary et al., 2017). Converely, Askary et al. (2017) reported different results. The antioxidant defense system of plants plays a crucial role in protecting against stressors. Increased SOD activity detoxifies O^{2-} into H_2O_2, which later converts to H_2O by the CAT activity. The activity of these enzymes enhances in response to Zn foliar treatment. It seems that Zn improved the CAT activity and reduced H_2O_2 accumulation (Wani et al., 2013; Al-Zahrani et al., 2021).

Superoxide dismutase (SOD) activity

The effects of salinity and foliar sprays affected the SOD activity ($p < 0.01$). The highest SOD activity was recorded with 50 and 100 mM salinity × all foliar sprays (Table 1). Table 1 shows the remarkable increase (76.6 %) in the SOD activity in $NaCl_{100}$ × nano-Zn compared to the control. Under salinity of 50 mM, the highest SOD activity was found in $NaCl_{50}$ × FeEDTA, which was 42 % higher than in $NaCl_{50}$ × no-foliar treatment. Nevertheless, other treatments, except for nano-Zn, showed a reduction of the SOD activity compared to the $NaCl_{100}$ × no-foliar treatment. The lowest SOD activity of this group of treatments was found in $NaCl_{100}$ × GO (38.7 % lower than $NaCl_{100}$ × no foliar). Zn foliar spray increased the SOD activity in lavender under 50 mM salinity compared to the same group controls (Chrysargyris et al., 2018). The application of GO improves the activity of antioxidant enzymes, helping thus in the survival and productivity under saline-sodic conditions (Safikhan et al., 2018; Gonzalez-Garcia et al., 2019). The Fe foliar treatment (Sequestrene 138 at a concentration of 5 per thousand) under saline conditions (90 mM) increased the SOD activity and thus stabilized the integrity of cell membranes in *Stevia rebaudiana* plants (Aghighi Shahverdi et al., 2018).

Phenolics and flavonoids contents

Total phenolics were affected by the independent effects of both salinity and foliar sprays ($p < 0.01$). Salinity of 50 and 100 mM improved the phenolic content (Figure 3). At salinity of 50 to 100 mM, the phenolic contents increased by 2.1 %. The foliar treatment with Chelated-Fe and magnetized-Fe increased the phenolic contents compared to other treatments (Table 2). Fe-treated plants had about 10 % more total phenolics than nano-Zn treated ones, indicating greater efficacy of Fe over Zn. The GO treatment attained higher phenolic contents than the control (77.8 mg g^{-1} FW compared to 64.8 mg g^{-1} FW), but with fewer effects on the phenolic contents than the mineral treatments.

Flavonoids were influenced by the independent effects of foliar sprays. The foliar spray with chelated-Fe increased the flavonoids content in tarragon. Compared to the Fe-EDTA treatment, there was a decrease of 6.2% and 7.5 % in the flavonoids content of nano-Zn and nano-Fe treated plants. The lowest flavonoids content (4.14 mg g^{-1}) was observed as a response to GO foliar spray (Table

2). Mahmoud et al. (2019) conducted a study on radish and found similar results. The authors reported that the foliar spray with nano-Fe raised the total phenolics and flavonoids contents in radish. Phenolics are essential secondary metabolites with key actions to scavenge the ROS molecules (Chrysargyris et al., 2018). The ability of phenolics to scavenge ROS depends on the number of aromatic rings and the identity of the revolving hydroxyl groups (Nickavar et al., 2005). Genetic variations and environmental features control the biosynthesis of phenolics in plants. The nutritional regime also has a key role in the biosynthesis of these compounds. The increase in the phenolics and flavonoids contents by the action of nano-Fe foliar treatments is possibly attributed to the enhanced photosynthesis potential and the partitioning of more assimilates and carbohydrates toward the shikimic acid pathway, thus intensifying the production and accumulation of the related secondary metabolites (Nickavar et al., 2005; Lingyun et al., 2016). The Zn treatment meliorates phenylalanine ammonia-lyase (PAL) activity in plants, fortifying the biosynthesis of phenolics and boosting plant endurance under stressful saline environments (Al-Zahrani et al., 2021).

Table 2 – Mean comparisons for the effects of foliar application (common and nano-zinc, FeEDTA and nano-iron and graphene oxide) on the elemental content and the total phenolics and flavonoids contents of Artemisia dracunculus plants grown in perlite.

Foliar spray	Flavonoids content	Total phenolics content	Na c ontent	K content	Fe content
	—— mg g^{-1} DWt ——		—— g kg^{-1} DWt ——		mg kg^{-1} DWt
No Foliar	5.1^{c}	64.8^{d}	12.2^{a}	9.6^{b}	29.1^{b}
Zinc oxide	6.4^{c}	83.8^{b}	10.4^{b}	8.6^{c}	25.5^{c}
Nano-zinc oxide	7.5^{b}	87.5^{b}	10.2^{b}	8.7^{c}	25.5^{c}
Fe EDTA	8^{a}	96.4^{a}	8.7^{c}	8.6^{c}	32.7^{ab}
Magnetic-Fe	7.4^{b}	92.1^{a}	8.5^{c}	8.9^{c}	37.4^{a}
Graphene oxide	4.1^{d}	77.8^{c}	8.7^{c}	12^{a}	33.2^{ab}

Differences ($p < 0.01$) between treatments are indicated by the different Latin letters.

Plant dry weight and plant height

The experimental treatment did not affect plant biomass ($p > 0.05$); however, salinity affected plant height and 50 mM salinity attained 10 % more data compared to the control (Figure 4). Further studies with broad concentration ranges of the foliar treatments are needed to explore in detail the effects the ranges on plant responses to yield.

Potassium and sodium contents and ratio

Salinity and foliar sprays influenced the K and Na contents ($p < 0.01$). With salinity up to 100 mM, the Na^+ content of samples increased (27 %) compared to the controls (Figure 5). Salinity influenced the K^+ content and the highest K^+ content was recorded in the control plants. With salinity of 100 mM, the K^+ content decreased by 22 % in relation to the control plants (Figure 5). The effects of foliar applications influenced the K^+ content in plants. The graphene foliar application raised the K^+ content (20 %) compared to the control treatment. The results showed no difference ($p > 0.01$) between Zn and Fe foliar applications in the K^+ content (Table 2). However, the K^+/Na^+ ratio was also responsive to salinity × foliar treatments (Table 1). The K^+/Na^+ ratio was affected by the interaction of treatments and the highest ratio was found in no-salinity × graphene foliar application. There was no difference ($p > 0.01$) between 50 and 100 mM salinity treatments and even with foliar applications (Table 1). Under saline environments, the ionic equilibrium is disrupted inside cells mainly by the over-uptake of Na^+ rather than K^+ and even by the interference on the actions of membrane-anchored carriers and transporters (Zhao et al., 2020). The Na^+ accumulation in the cytoplasm causes toxic effects on cell metabolism mainly via the partial substitution of K^+ specific domains by Na^+ and the subsequent side effects on cell metabolism (Zhao et al., 2020). Na^+ accumulation in plants has destructive effects on photosynthesis, on the N content, and on the amino

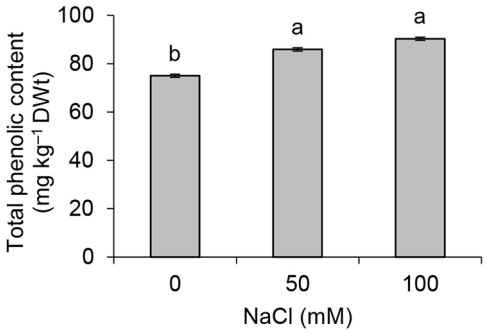

Figure 3 – Mean comparison for the effects of NaCl salinity (0, 50, and 100 mM) on the total phenolics content of *Artemisia dracunculus* plants grown in perlite. Differences ($p < 0.01$) between treatments are indicated by the diverse Latin letters.

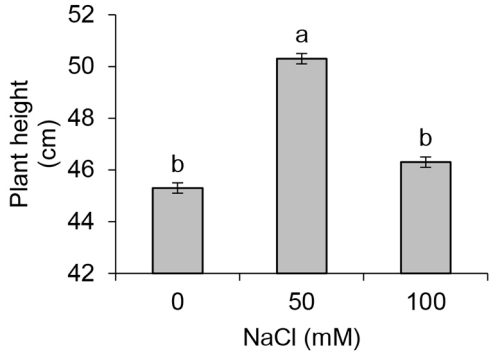

Figure 4 – Mean comparison for the effects of NaCl salinity (0-50 and 100 mM) on the height of *Artemisia dracunculus* plants grown in perlite. Differences ($p < 0.01$) between treatments are indicated by the diverse Latin letters.

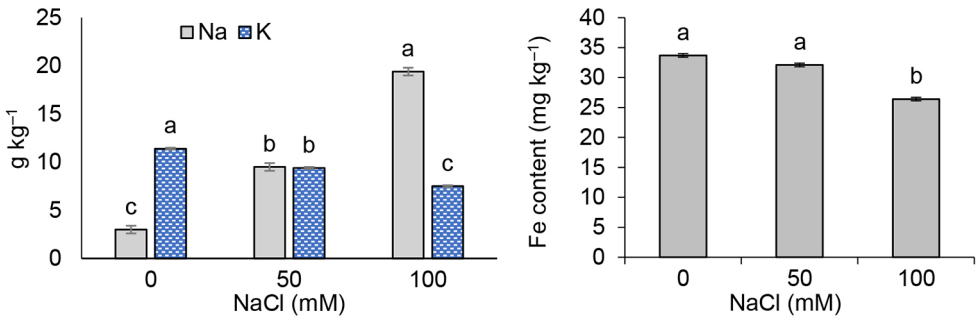

Figure 5 – Mean comparisons for the effects of NaCl salinity (0-50 and 100 mM) on the contents of Na, K, and Fe of *Artemisia dracunculus* plants grown in perlite. Differences ($p < 0.01$) between treatments are indicated by the diverse Latin letters.

acids biosynthesis (Munns and Tester, 2008; Piñero et al., 2019). The increased K^+ content in the plants grown in a saline environment is a canonical factor that shows salinity tolerance in plants. K^+ availability plays a key role in the osmotic potential regulation of root cells, in the translocation of solutes in the xylem, and in water equilibrium of plants (Munns and Tester, 2008).

The Zn foliar application positively effectsK^+ absorption and metabolism thereby maintaining the integrity of cell membranes and withstanding photosynthesis under stressful conditions (Tufail et al., 2018). Foliar application in our experiment amended the absorption of essential nutrients, especially K^+, favoring balanced growth and development as well as stress tolerance. However, Fe foliar spray of peppermint under salinity of 150 mM was not able to prevent Na^+ over-accumulation and/or to increase the K^+ content (Askary et al., 2017). The K^+ content and the K^+/Na^+ ratio in rosemary were positively influenced by the foliar treatment of nano-Fe and Zn under salinity. Therefore, with salinity up to 225 mM, foliar treatment did not keep the K/Na ratios (Hassanpouraghdam et al., 2019).

Fe and Zn ions content

The Fe content was responsive to the effects of salinity and foliar sprays. The foliar application of GO, magnetic Fe, and chelated Fe influenced the Fe content of plants ($p < 0.05$). The lowest Fe content was found in Zn-foliar treated plants (Table 2). The highest Fe content was recorded with the control plants (no salinity treatment) and in pots exposed to 50 mM salinity (Figure 5).

The Zn content was influenced by the interaction effects of treatments. The highest Zn^{2+} content was recorded in the experiment of no salinity × foliar spray with Zn-oxide and nano-zinc (81 and 82 % more than control) (Table 1). In rosemary, the Zn and Fe contents were responsive to the interactions of salinity × foliar sprays and the highest Fe content was recorded in the no salinity × Fe foliar treatment. The highest Zn content was recorded with no saline conditions × Zn foliar use. Salinity progression of up to 225 mM reduced the Fe and Zn contents in leaves (39 and 30 %, respectively compared to control plants) (Vojodi Mehrabani et al., 2018; Hassanpouraghdam et al., 2019). Here, we observed a declining pattern for the Zn content with increasing salinity levels (up to 100 mM). Under salinity conditions, Zn application may alleviate the possible Na^+ and Cl^- injury in plants by mitigating the adverse effect of NaCl and mostly by inhibiting Na and/or Cl uptake or translocation (Parker et al., 1992). Furthermore, the results indicate that the Fe and GO foliar treatments improved the Fe contents in plants (Table 2). In peppermint, nano-Fe foliar application increased the Fe content in plant tissues (Askary et al., 2017). Fe has a functional role in chlorophylls and thylakoids syntheses and chloroplast development as well as in cell metabolisms, such as the activation of some enzymes associated to superoxide dismutase and carbohydrate pathway (Marschner, 1995; Mahmoud et al., 2019).

Essential oil constituents

The gas chromatography-mass spectrometry (GC/MS) analysis showed the occurrence of 38 compounds in the oil of *A. dracunculus* (Table 3). Estragole (81-91.8 %) was the most dominant constituent in all the treatments. Plants submitted to 50 and 100 mM NaCl treatments sprayed with ZnO, presented the highest estragole content (3.8 % higher than the control and 2.3 and 8.9 % higher than 50 and 100 mM NaCl without ZnO). The lowest estragole content was recorded with 100 mM NaCl with FeEDTA foliar application. The other major constituent was limonene (1-2.6 %). The $NaCl_{100\ mM}$ × GO and FeEDTA foliar spray had 42 and 44 % more limonene than the control plant. The results showed that foliar application with GO and FeEDTA increase the limonene content by 22.5 % compared to $NaCl_{100}$ × non-foliar application. Cis-ocimene (0.1-6.4 %) presented a high variation among the treatments. The highest data for cis-ocimene was recorded at $NaCl_{100\ mM}$ × Fe-chelated foliar spray (6.4 %) and GO (6.1 %) treatments, which showed an increase of 61.6 % and 63.5 %, respectively, compared to the control. The highest amount of methyl eugenol (1-2.5 %) was observed with $NaCl_{50\ mM}$ × no foliar spray and 100 mM salinity with ZnO foliar application

Table 3 – Essential oil composition of *Artemisia dracunculus* plants exposed to salinity and foliar applications of diverse Fe and Zn sources and graphene oxide.

Components	RT	RI	V1	V2	V3	V4	V5	V6	V7	V8	V9	V10	V11	V12	V13	V14	V15	V16	V17
α-Pinene	8.773	1030	0.452	0.408	0.323	0.322	0.423	0.417	0.917	0.722	0.546	0.648	0.59	0.301	0.636	0.462	0.461	0.355	0.517
β-Pinene	10.885	1119	0	0	0	0	0	0	0.115	0.096	0.072	0.089	0.082	0	0.086	0.074	0	0	0.076
Sabinene	11.205	1129	0	0	0	0	0	0	0.081	0.07	0	0.064	0.082	0	0.063	0	0	0	0
β-Myrcene	12.355	1166	0.072	0.068	0	0	0	0	0.11	0.102	0.081	0.097	0	0	0.088	0.075	0	0	0.075
dl-Limonene	13.711	1208	1.684	1.866	1.569	1.261	1.38	1.48	2.669	2.56	2.169	2.36	2.068	1.064	2.173	1.946	1.298	1.113	1.953
cis-Ocimene	14.867	1238	4.901	4.577	2.749	0.141	0.879	2.345	6.1	6.421	5.443	5.818	4.687	0.374	5.229	4.513	2.126	1.919	4.133
β-Ocimene	15.531	1256	2.996	3.019	1.503	0	0.339	1.24	3.864	4.43	3.688	3.813	3.002	0.127	3.464	3.009	1.061	1.034	2.585
m-Cymene	16.412	1279	0.079	0	0	0	0	0	0	0	0	0	0	0	0	0	0	0	0
3-Octyne, 2-methyl-	19.748	1362	0	0	0.135	0.157	0.169	0.14	0.089	0	0	0.073	0.098	0.133	0.072	0.074	0.114	0.084	0.109
Neo-allo-ocimene	20.389	1378	0.127	0.117	0	0	0	0	0.156	0.167	0.137	0.151	0.126	0	0.137	0.114	0	0	0.105
3-Octyne, 7-methyl-	21.327	1401	0	0	0.139	0.16	0.17	0.139	0.092	0	0	0.073	0.101	0.144	0	0.082	0.121	0.094	0.118
cis-Ocimene oxide	25.075	1493	0	0	0.078	0	0	0.085	0	0	0	0	0	0	0	0	0	0	0
(-)-Bornyl acetate	28.874	1588	0.126	0.146	0.173	0.237	0.216	0.205	0.142	0.119	0.105	0.118	0.149	0.158	0.134	0.157	0.188	0.185	0.165
6-Methyl-3,5-heptadien-2-one	29.315	1599	0	0	0.09	0.134	0.144	0.125	0	0	0	0	0	0	0	0	0	0	0
Caryophyllene	29.595	1606	0.167	0.122	0.125	0	0.092	0.149	0.113	0.162	0.19	0.134	0.134	0	0.144	0.117	0.139	0.199	0.139
Carvacrol methyl ether	29.727	1610	0.12	0	0	0	0	0	0	0	0	0	0	0	0	0	0	0	0
Estragole	32.382	1680	83.865	86.176	88.444	91.82	89.258	87.873	81.557	81.024	82.388	82.136	84.551	91.429	83.671	85.586	88.822	88.666	85.353
Germacrene D	33.83	1718	0.36	0.21	0.155	0	0	0.127	0.221	0.363	0.386	0.263	0.248	0	0.278	0.235	0.139	0.201	0.221
(E,Z)-α-Farnesene	34.196	1728	0.494	0.38	0.401	0	0.184	0.353	0.353	0.511	0.532	0.422	0.426	0	0.416	0.385	0.366	0.517	0.407
Bicyclogermacrene	34.711	1741	0.394	0.131	0	0	0	0	0.142	0.441	0.395	0.212	0.159	0	0.21	0.153	0	0	0.141
(E,E)-α-Farnesene	35.048	1750	0.087	0	0	0	0	0	0	0.098	0.108	0.082	0.086	0	0.088	0	0	0	0
β-Sesquiphellandrene	35.941	1774	0.087	0.137	0.216	0	0.129	0.184	0.144	0.176	0.233	0.167	0.172	0	0.163	0.178	0.211	0.248	0.201
4,5–epoxy-1-isopropyl-4-methyl-1-cyclohexene	37.829	1821	0.237	0.205	0.168	0	0	0.168	0.234	0.184	0.219	0.238	0.223	0	0.23	0.219	0.134	0.141	0.212
(-)-Caryophyllene oxide	44.656	1993	0	0	0	0.164	0.144	0	0	0	0	0	0	0.172	0	0	0	0	0
Cyclopentane, 1,1'-ethylidenebis-	45.005	2003	0.089	0.09	0.108	0.101	0.12	0.131	0.104	0	0	0.077	0.098	0	0.098	0.077	0.093	0.085	0.111
Methyl eugenol	45.382	2017	1.372	1.356	1.605	2.268	2.547	2.294	1.561	1.255	1.554	1.411	1.475	2.463	1.318	1.348	2.288	2.214	1.466
Anisaldehyde	45.891	2034	0	0	0.128	0.818	0.366	0.199	0	0	0	0	0	0.527	0	0	0.176	0.121	0
Phenylpropanamide	46.87	2069	0	0	0	0	0.13	0	0	0	0	0	0	0	0	0	0	0	0.177
(+)-Spathulenol	48.478	2131	0.477	0.583	0.929	1.182	1.472	1.189	0.659	0.478	0.728	0.677	0.722	1.352	0.693	0.618	1.105	1.281	0.711
o-Allylphenol	48.615	2137	0	0	0	0	0.074	0.082	0	0	0	0	0	0	0	0	0	0	0
Vinyltrimethylsilane	49.062	2156	0	0	0	0.077	0.102	0	0	0	0	0	0	0.087	0	0	0.067	0.093	0
Octaethylene glycol monododecyl ether	49.491	2174	0	0	0.064	0.1	0.088	0	0.063	0	0.075	0.081	0	0.101	0	0	0	0	0
Thymol	49.794	2187	0.359	0	0	0	0	0	0	0	0	0	0	0	0	0	0	0	0
Carvacrol	50.441	2216	0.929	0.065	0.123	0	0	0	0	0	0	0	0	0	0	0	0	0	0.221
Isospathulenol	50.778	2233	0	0	0.086	0.127	0.083	0.14	0.083	0.074	0.105	0.078	0.077	0.112	0.071	0.073	0.098	0.142	0.079
Acenaphthene	51.139	2251	0	0	0	0	0	0.276	0	0	0	0	0	0	0.104	0	0	0	0
Germacyclobutane, 1,1-dimethyl-	51.379	2263	0	0.091	0.132	0.144	0.213	0.169	0.093	0.097	0.142	0.109	0.13	0.206	0	0.103	0.166	0.21	0.119
Phytol	57.456	2613	0.528	0.254	0.556	0.788	1.274	0.49	0.337	0.45	0.706	0.612	0.515	1.251	0.433	0.404	0.828	1.1	0.605

V1 = $NaCl_0$ + graphene oxide; V2 = $NaCl_{50mM}$ + ZnO;V3 = $NaCl_0$ + nano ZnO; V4 = $NaCl_{100\ mM}$ + ZnO; V5 = $NaCl_{50mM}$ + no foliar application; V6 = $NaCl_0$ + no foliar application; V7 = $NaCl_{100mM}$ + graphene oxide; V8 = $NaCl_{100mM}$ + FeEDTA; V9 = $NaCl_{100mM}$ + nano ZnO; V10 = $NaCl_0$ + ZnO; V11 = $NaCl_0$ + FeEDTA; V12 = $NaCl_{50mM}$ + ZnO; V13 = $NaCl_{100}$ + no foliar application; V14 = $NaCl_0$ + nano Fe; V15 = $NaCl_{50mM}$ + nano Fe; V16 = $NaCl_{50mM}$ + graphene oxide; V17 = $NaCl_{50mM}$ + FeEDTA.

with an increase of 44 % and 9 %, respectively, compared to the control plants (Table 3). Salinity increased the oil content by motivating enzymes involved in the terpenoids and phenylpropanoids pathway in plants (Sharma et al., 2019). Besides, any interference in photosynthesis and carbohydrates production indirectly affects the oil content and the compositional profile in the essential oil-bearing plants (Gohari et al., 2020a, b). Previous reports indicated that the biosynthesis of monoterpenes is more affected by salinity than of sesquiterpenes. Overall, biosynthesis and accumulation of monoterpenes are more responsive and sensitive to salinity (Turner and Croteau, 2004). In *Mentha piperita* L., foliar spray with nano-Fe × $NaCl_0$ increased the oil content and the percentage of menthone and pulegone. The salinity conditions and no foliar spray increased the amounts of menthol and menthofuran (Askary et al., 2017). EOs have diverse plant functions, such as protection against pests and diseases, the attraction of pollinators, and deterrent actions against herbivores and fungal infections (Laranjo et al., 2019). Even though the genetic heritage controls oil biosynthesis,, environmental stimuli greatly affect the biosynthesis of essential oils (Laranjo et al., 2019). Zn plays crucial functions in photosynthesis and in the metabolism of carbohydrates with indirect dominant roles in the EOs biosynthesis. Furthermore, Said-Al Ahl and Mahmoud (2010) reported that the use of Zn and Fe in basil production increased the amounts of linalool, sabinene, eugenol, and cadinole.

Conclusion

Given the extension of agricultural areas prone to salinization and the aim to increase arability in these areas, ameliorative methods to reduce the salinity effects on plant growth and yield deserve great attention. In our study, salinity did not influence the yield of tarragon. The foliar treatments were relatively promising to reduce the perilous salinity effects. The K/Na ratio, a major salinity tolerance marker, was positively affected by the GO treatment. The antioxidant enzymes were more responsive to salinity than the foliar treatments. Accumulation of EOs in plant tissues was accelerated with Zn under salinity. The oil constituents were variably impacted by the interaction of salinity and foliar sprays and the variation range was constituent-dependent. The foliar treatments seemed to partially ameliorate the salinity adverse effects on plants. Studies with more details and a broad range of foliar treatment concentrations should provide advisable results extension sections under greenhouse production systems. Further in-depth studies are necessary to decide on field growing conditions.

Acknowledgments

This study was financially supported by the Azarbaijan Shahid Madani University, Tabriz, Iran, and the University of Maragheh, Iran. These results were from MSc thesis of Mrs. Nahideh Kheirollahi.

Authors' Contributions

Conceptualization: Mohammad, B.H.; Lamia, V.M. **Data acquisition:** Lamia, V.M.; Mohammad, B.H.; Nahideh, K.; Amir, S. **Design of methodology:** Mohammad, B.H.; Lamia, V.M.; Amir, S.; Leila, K.; Nahideh, K. **Writing and editing:** Lamia, V.M.; Mohammad, B.H.; Nahideh, K.

References

Adams, R.P. 2007. Identification of essential oil components by gas chromatography/ mass spectrometry. 4ed. Allured Publishing, Carol Stream, IL.

Aghighi Shahverdi, M.; Omidi, H.; Tabatabaei, S.J. 2018. Effects of foliar application of selenium, boron and iron on some physiological traits and glycoside of stevia (*Stevia rebaudiana* Bertoni) under salinity stress. Iranian Journal of Medicinal and Aromatic Plants 33: 1017-1033. http://dx.doi.org/10.22092/IJMAPR.2018.114425.2067

Ahmad, P.; Ahanger, M.A.; Alyemeni, M.N.; Wijaya, L.; Egamberdieva, D.; Bhardwaj, R.; Ashraf, M. 2017. Zinc application mitigates the adverse effects of NaCl stress on mustard [*Brassica juncea* (L.) Czern & Coss] through modulating compatible organic solutes, antioxidant enzymes, and flavonoid content. Journal of Plant Interactions 12: 429-437. https://doi.org/10.1080/17429145.2017.1385867

Al-Zahrani, H.S.; Alharby, H.F.; Hakeem, K.R.; Ul Rehman, R. 2021. Exogenous application of zinc to mitigate the salt stress in *Vigna radiata* L. Wilezek- evaluation of physiological and biochemical processes. Plants 10: 1005. https://doi.org/10.3390/plants10051005

Anjum, N.A.; Singh, N.; Singh, M.K.; Sayeed, I.; Duarte, A.C.; Pereira, E.; Ahmad, I. 2014. Single-bilayer graphene oxide sheet impacts and underlying potential mechanism assessment in germinating faba bean (*Vicia faba* L.). Science of The Total Environment 472: 834-841. https://doi.org/10.1016/j.scitotenv.2013.11.018

Antoniou, C.; Savvides, A.; Christou, A.; Fotopoulos, V. 2016. Unraveling chemical priming machinery in plants: the role of reactive oxygen-nitrogen-sulfur species in abiotic stress tolerance enhancement. Current Opinion in Plant Biology 33: 101-107. https://doi.org/10.1016/j.pbi.2016.06.020

Askary, M.; Talebi, S.M.; Amini, F.; Bangan, A.D.B. 2017. Effects of iron nanoparticles on *Mentha piperita* L. under salinity stress. Biologija 63: 65-75. https://doi.org/10.6001/biologija.v63i1.3476

Begurn, P.; Ikhtiari, R.; Fugetsu, B. 2011. Graphene phytotoxicity in the seeding stage of cabbage, tomato, red spinach, and lettuce. Carbon 49: 3907-3919. https://doi.org/10.1016/j.carbon.2011.05.029

Camel, V. 2003. Solid-phase extraction of trace elements. Spectrochimica Acta Part B Atomic Spectroscopy 58: 1177-1233. https://doi.org/10.1016/S0584-8547(03)00072-7

Cheng, F.; Liu, Y.F.; Lu, G.Y.; Zhang, X.K.; Xie, L.L.; Yuan, C.F.; Xu, B.B. 2016. Graphene oxide modulates root growth of *Brassica napus* L.and regulates ABA and IAA concentration. Journal of Plant Physiology 193: 57-63. https://doi.org/10.1016/j.jplph.2016.02.011

Chrysargyris, A.; Michailidi, E.; Tzortzakis, N. 2018. Physiological and biochemical responses of *Lavandula angustifolia* to salinity under the mineral foliar application. Frontiers in Plant Science 9: 489. https://doi.org/10.3389/fpls.2018.00489

Deng, S.; Berry, V. 2016. Wrinkled, rippled and crumpled graphene: an overview of formation mechanism, electronic properties, and applications. Materials Today 19: 197-212. https://doi.org/10.1016/j.mattod.2015.10.002

Drazkiewicz, A. 1994. Chlorophyllase: occurrence, functions, mechanism of action, effects of external and internal factors. Photosynthetica 30: 321-331.

El Mokhtari, A.; Cabassa-Hourton, C.; Farissi, M.; Savoure, A. 2020. How does proline treatment promote salt stress tolerance during crop plant development? Frontiers in Plant Science 11: 1127. https://doi.org/10.3389/fpls.2020.01127

Etesami, H.; Fatemi, H.; Rizwan, M. 2021. Interaction of nanoparticles and salinity stress at physiological, biochemical and molecular levels in plants. A review. Ecotoxicology and Environmental Safety 225: 112769. https://doi.org/10.1016/j.ecoenv.2021.112769

Fedina, I.; Georgieva, K.; Velitchkova, M.; Grigorova, I. 2006. Effect of pretreatment of barley seedlings with different salts on the level of UV-B induced and UV-B absorbing compounds. Environmental and Experimental Botany 56: 225-230. https://doi.org/10.1016/j.envexpbot.2005.02.006

Giannopolitis, C.N.; Ries, S.K. 1977. Superoxide dismutase. II. Purification and quantities relationship with water-soluble protein in seedling. Plant Physiology 59: 315-318. https://doi.org/10.1104/pp.59.2.315

Gohari, G.; Zareei, E.; Rostami, H.; Panahirad, S.; Kulak, M.; Farhadi, H.; Amini, M.; Martinez-Ballesta, M.C.; Fotopoulou, V. 2021. Protective effects of cerium oxide nanoparticle in grapevine (*Vitis vinifera* L.) cv. Flame seedless under salt stress conditions. Ecotoxicology and Environmental Safety 220. https://doi.org/10.1016/j.ecoenv.2021.112402

Gohari, G.; Mohammadi, A.; Akbari, A.; Panahirad, S.; Dadpour, M.R.; Fotopoulous, V.; Kimura, S. 2020a. Titanium dioxide nanoparticles (TiO_2 NPs) promote growth and ameliorate salinity stress effects on essential oil profile and biochemical attributes of *Dracocephalum moldavica*. Scientific Reports 10: e912 https://doi.org/10.1038/s41598-020-57794-1

Gohari, G.; Alavi, Z.; Esfandiari, E.; Panahirad, S.; Hajihoseinlou, S.; Fotopoulos, V. 2020b. Interaction between hydrogen peroxide and sodium nitroprusside following chemical priming of *Ocimum basilicum* L. against salt stress. Physiologia Plantarum 168:361-373. https://doi.org/10.1111/ppl.13020

Gonzalez-Garcia, Y.; Lopez-Vargas, E.R.; Cadenas-Pliego, G.; Benavides-Mendoza, A.; Gonzalez-Morales, S.; Robledo-Olivo, A.; Alpuche-Solis, A.G.; Juarez-Maldonado, A. 2019. Impact of carbon nanomaterials on the antioxidant system of tomato seedling. International Journal of Molecular Science 20: 5858. https://doi.org/10.3390/ijms20235858

Guo, H.; Huang, Z.; Li, M.; Hou, Z. 2020. Growth, ionic homeostasis, and physiological responses of cotton under different salt and alkali stress. Scientific Reports 10: 21844. https://doi.org/10.1038/s41598-020-79045-z

Hassanpouraghdam, M.B.; Gohari, G.R.; Tabatabaei, S.J.; Dadpour, M.R.; Shirdel, M. 2010. NaCl salinity and Zn Foliar application influence essential oil composition of basil (*Ocimum basilicum* L.). Acta Agriculturae Slovenica 97: 93-98. https://doi.org/10.2478/v10014-011-0004-x

Hassanpouraghdam, M.B.; Vojodi Mehrabani, L.; Tzortzakis, N. 2019. Foliar application of Nano-Zinc and Iron affects physiological attributes of *Rosmarinus officinalis* and quietens NaCl salinity depression. Journal of Soil Science and Plant Nutrition 20: 335-345. https://doi.org/10.1007/s42729-019-00111-1

Honarjoo, N.; Hajrasuliha, Sh.; Amini, H. 2013. Comparing three plants in absorption of ions from different natural saline and sodic soils. International Journal of Agriculture and Crop Sciences 6: 988-993.

Kanjana, D. 2019. Foliar study on effect of iron oxide nanoparticles as an alternate source of iron fertilizer to cotton. International Journal of Chemical Studies 7: 4374-4379.

Kim, K.H.; Tsao, R.; Yang, R.; Cui, S.W. 2006. Phenolic acid profiles and antioxidant activities of wheat bran extracts and the effect of hydrolysis conditions. Food Chemistry 95: 466-473. https://doi.org/10.1016/j.foodchem.2005.01.032

Kordali, S.; Kotan, R.; Mavi, A.; Cakir, A.; Ala, A.; Yildrim, A. 2005. Determination of the chemical composition and antioxidant activity of the essential oil of *Artemisia dracunculus* and of the antifungal and antibacterial activities of Turkish *Artemisia absinthium*, *A. dracunculus, Artemisia santonicum,* and *Artemisia spicigera* essential oils. Journal of Agricultural and Food Chemistry 53: 9452-9458. https://doi.org/10.1021/jf0516538

Laranjo, M.; Fernandez-leon, A.M.; Agulheiro-Santos, A.C.; Potes, M.E.; Elias, M. 2019. Essential oils of aromatic and medicinal plants play a role in food safety. Journal of Food Processing and Preservation: e14278. https://doi.org//10.1111/jfpp.14278

Lingyun, Y.; Jian, W.; Chenggang, W.; Shan, L.; Shidong, Z. 2016. Effect of zinc enrichment on growth and nutritional quality in pea sprouts. Journal of Food and Nutrition Research 4: 100-107. https://doi.org/10.12691/jfnr-4-2-6

Luhova, L.; Lebeda, A.; Hederorva, D.; Pec, P. 2003. Activities of amine oxidase, peroxidase and catalase in seedlings of *Pisum sativum* L. under different light conditions. Plant, Soil and Environment 49: 151-157. https://doi.org/10.17221/4106-PSE

Mahmoud, A.W.; Abdelaziz, S.M.; EL-Mogy, M.M.; Abdeldaym, E.A. 2019. Effect of foliar ZnO and FeO nanoparticles application on growth and nutritional quality of red radish and assessment of their accumulation on human health. Agriculture (Po'nohospodárstvo) 65: 16-29. https://doi.org/10.2478/agri-2019-0002

Mahmoud, N.E.; Abdelhameed, R.M. 2021. Superiorities of modified graphene oxide for enhancing the growth, yield and antioxidant potential of pearl millet (*Pennisetum glaucum* L.) under salt stress. Plant Stress 2: 100025. https://doi.org/10.1016/j.stress.2021.100025

Mansour, M.M.F.; Ali, E.F. 2017. Evaluation of proline functions in saline conditions. Phytochemistry 140: 52-68. https://doi.org/10.1016/J.PHYTOCHEM.2017.04.016

Marschner, H. 1995. Mineral Nutrient of Higher Plants. 2ed. Academic Press, London, UK.

Munns, R.; Tester, M. 2008. Mechanisms of salinity tolerance. Annual Review of Plant Biology 59: 651-681. https://doi.org/10.1146/annurev.arplant.59.032607.092911

Nakajima, T.; Mabuchi, A.; Hagiwara, R. 1988. A new structure model of graphite oxide. Carbon 26: 357-361. https://doi.org/10.1016/0008-6223(88)90227-8

Nareshkumar, A.; Veeranagamallaiah, G.; Pandurangaiah, M.; Kiranmai, K.; Amaranathareddy, V.; Lokesh, U.; Venkatesh, B.; Sudhakar, C. 2015. Pb-stress induced oxidative stress caused alterations in antioxidant efficacy in two groundnuts (*Arachis hypogaea* L.) cultivars. Agricultural Sciences 6: 1283-1297. https://doi.org/10.4236/as.2015.610123

Nickavar, B.; Mojab, F.; Dolat-Abadi, R. 2005. Analysis of the essential oils of two Thymus species from Iran. Food Chemistry 90: 609-611. https://doi.org/10.1016/j.foodchem.2004.04.020

Nieves-Cordones, M.; Aleman, F.; Martinez, V.; Rubio, F. 2010. The *Arabidopsis thaliana* HAK5 K^+ transporter is required for plant growth and K^+ acquisition from low K^+ solutions under saline conditions. Molecular Plant 3: 326-333. https://doi.org/10.1093/mp/ssp102

Pandey, K.; Lahiani, M.H.; Hicks, V.K.; Hudson, M.K.; Green, M.J.; Khodakovskaya, M. 2018. Effects of carbon-based nanomaterials on seed germination, biomass accumulation and salt stress response of bioenergy crops. Plos One 13: e0202274. https://doi.org/10.1371/journal.pone.0202274

Parker, D.R.; Aguilera, J.J.; Thomason, D.N. 1992. Zinc-phosphorus interactions in two cultivars of tomato (*Lycopersicon esculentum* L.) grown in chelator-buffered nutrient solutions. Plant and Soil 143: 163-177. https://doi.org/10.1007/BF00007870

Piñero, M.C.; Porras, M.E.; López-Marín, J.; Sánchez-Guerrero, M.C.; Medrano, E.; Lorenzo, P.; del Amor, F.M. 2019. Differential nitrogen nutrition modifies polyamines and the amino-acid profile of sweet pepper under salinity stress. Frontiers in Plant Science 10: 301. https://doi.org/10.3389/fpls.2019.00301

Obolskiy, D.; Pischel, I.; Feistel, B.; Glotov, N.; Heinrich, M. 2011. *Artemisia dracunculus* L. (Taragon): a critical review of its traditional use, chemical composition, pharmacology, and safety. Journal of Agricultural and Food Chemistry 59: 11367-11384. https://doi.org/10.1021/jf202277w

Quettier-Deleu, C.; Gressier, B.; Vasseur, J.; Dine, T.; Brunet, C.; Luyckx, M.; Cazin, M.; Cazin, J.C.; Bailleul, F.; Trotin, F. 2000. Phenolic compounds and antioxidant activities of buckwheat (*Fagopyrum esculentum* Moench) hulls and flour. Journal of Ethnopharmacology 72: 35-42. https://doi.org//10.1016/S0378-8741(00)00196-3

Rady, M.M.; Sadak, M.Sh.; El-Bassiouny, H.M.S.; Abd El-Monem, A.A. 2011. Alleviation of the adverse effects of salinity stress in sunflower cultivars using nicotinamide and α-tocopherol. Australian Journal of Basic and Applied Sciences 5: 342-355.

Ren, W.; Chang, H.; Teng, Y. 2016. Sulfonated graphene-induced hormesis is mediated through oxidative stress in the roots of maize seedlings. Science of The Total Environment 572: 926-934. https://doi.org/10.1016/j.scitotenv.2016.07.214

Safikhan, S.; Chaichi, M.R.; Khoshbakht, K.; Amini, A.; Motesharezadeh, B. 2018. Application of nanomaterial graphene oxide on biochemical traits of milk thistle (*Silybum marianum* L.) under salinity stress. Australian Journal of Crop Science 12: 931-936. https://doi.org/10.21475/ajcs.18.12.06.PNE972

Said-Al Ahl, H.A.H.; Mahmoud, A.A. 2010. Effect of zinc and/or iron foliar application on growth and essential oil of sweet basil (*Ocimum basilicum* L.) under salt stress. Ozean Journal of Applied Sciences 3: 97-111. Available at: https://www.researchgate.net/publication/228443153 [Accessed Jan 15, 2010]

Santander, C.; Sanhueza, M.; Olave, J.; Borie, F.; Valentine, A.; Cornejo, P. 2019. *Arbuscular mycorrhizal* colonization promotes the tolerance to salt stress in lettuce plants through an efficient modification of ionic balance. Journal of Soil Science and Plant Nutrition 19: 321-331. https://doi.org/10.1007/s42729-019-00032-z

Shahriary, L.; Athawale, A.A. 2014. Graphene oxide synthesized by using modified hummers approach. International Journal of Renewable Energy and Environmental Engineering 2: 58-63. Available at: https://www.researchgate.net/publication/303044105 [Accessed Jan 10, 2014]

Sharma, A.; Shahzad, B.; Rehman, A.; Bhardwaj, R.; Landi, M.; Zheng, B. 2019. Response of phenylpropanoid pathway and the role of polyphenols in plants under abiotic stress. Molecules 24: 2452. https://doi.org/10.3390/molecules24132452

Tufail, A.; Li, H.; Naeem, A.; Li, T.X. 2018. Leaf cell membrane stability-based mechanisms of zinc nutrient in mitigating salinity stress in rice. Plant Biology 20: 338-345. https://doi.org/10.1111/plb.12665

Turner, G.W.; Croteau, R. 2004. Organization of monoterpene biosynthesis in Mentha: Immunocytochemical localization of geranyl diphosphate synthase, limonene-6-hydroxylase, isopiperitenol dehydrogenase, and pulegone reductase. Plant Physiology 136: 4215-4227. https://doi.org/10.1104/pp.104.050229

Vojodi Mehrabani, L.; Hassanpouraghdam, M.B.; Shamsi-Khotab, T. 2018. The effects of common and nano-zinc foliar application on the alleviation of salinity stress in *Rosmarinus officinalis* L. Acta Scientiarum Polonorum Hortorum Cultus 17: 65-73. https://doi.org/10.24326/asphc.2018.6.7

Wani, A.S.; Ahmad, A.; Hayat, S.; Fariduddin, Q. 2013. Salt-induced modulation in growth, photosynthesis and antioxidant system in two varieties of *Brassica juncea*. Saudi Journal of Biological Science 20: 183-193. https://doi.org/10.1016/j.sjbs.2013.01.006

Wu, C.A.; Yang, G.D.; Meng, Q.W.; Zheng, C.C. 2004. The cotton GhNHX1 gene encoding a novel putative tonoplast Na^+/H^+ anti-porter plays an important role in salt stress. Plant and Cell Physiology 45: 600-607. https://doi.org/10.1093/pcp/pch071

Zhao, C.; Zhang, H.; Song, C.; Zhu, J.K.; Shabala, S. 2020. Mechanisms of plant responses and adaptation to soil salinity. The Innovation 1: 100017. https://doi.org/10.1016/j.xinn.2020.100017